g-C$_3$N$_4$ Decorated TiO$_2$ Nanotube Ordered Thin Films as Cathodic Electrodes for the Selective Reduction of Oxalic Acid

Federica De Luca, Rosalba Passalacqua*, Francesco P. Abramo, Siglinda Perathoner, Gabriele Centi, Salvatore Abate*

Departments of ChiBioFarAM and MIFT, University of Messina, ERIC aisbl and INSTM/CASPE, V.le F. Stagno d'Alcontres 31, Messina 98166, Italy
abates@unime.it ; rpassalacqua@unime.it

A new value chain in carbon dioxide utilization is the production of high-added-value C2 products from CO$_2$ via oxalic acid as intermediate. We report here the use of novel g-C$_3$N$_4$ decorated TiO$_2$ nanotube ordered thin films as cathodic electrodes for the selective reduction of oxalic acid to high-added-value chemicals such as glyoxylic acid and glycolic acid. These electrodes have been tested in a three-electrode electrocatalytic cell, using 0.2 M Na$_2$SO$_4$ as electrolyte, at applied potentials of -1.1 and -1.3 V vs Ag/AgCl. The cathode side of the continuous electrocatalytic cell is feed with a solution of 0.03 M oxalic acid (OX). Glycolic acid (GC) and glyoxylic acid (GO) have been obtained as the main reaction products. g-C$_3$N$_4$ was deposited on the pristine TiO$_2$ nanotube ordered array thin film (on a metallic Ti substrate acting as conductive element) by a modified chemical vapor deposition technique, varying the experimental parameters to obtain a series of materials. The pristine TiO$_2$ nanotubes gives faradaic efficiency (FE) to GO and GC of 24%, and 34%, respectively, while after decoration of TiO$_2$ nanotubes with g-C$_3$N$_4$ a large change in FEs is observed, depending on the specific characteristics of deposition, while the current density remains nearly constant. The FE to GC reaches at the best a value of 76% while the FE to GO is lowered to 12%. The preliminary interpretation of this drastic modification of the behaviour is related to the effect of g-C$_3$N$_4$ induced on the properties of TiO$_2$ nanostructured film.

1. Introduction

The development of new routes for the utilization of CO$_2$ emissions is a current hot topic to comply with political targets for reduction of greenhouse gas emissions and energy transition. Electrocatalytic reduction of CO$_2$ offers the possibility to combine the utilization of renewable energy sources to the direct utilization of CO$_2$ to form valuable chemicals/fuels (Perathoner and Centi, 2019). However, it is necessary to expand the value chain in CO$_2$ utilization, by addressing novel possibilities related to the formation of C2 rather than C1 products, the latter being the most studied currently. This is the focus of the OCEAN EU project, which objective is to develop industrial process at demo scale for the conversion of CO$_2$ to oxalic acid (OX) as intermediate, further converted (electrocatalytically) to various high value C$_2$ products, of relevance particularly as monomers for polymers.

Murcia Valderrama et al. (2019) have discussed in detail the potential of oxalic – and glycolic acids (GC) to produce novel polyesters. In addition, the interest towards GC and its derivates is motivated by use in several industries of α-hydroxy acid. It is used in the textile industry as a whitener and tanning agent, in the food industry as a flavoring and preservative; as a monomer for the synthesis of polyglycolic acid (PGA), a biodegradable and thermoplastic polymer and the simplest member of the aliphatic linear polyester family.

$$OX \xrightarrow{2H^+,2e^-} GO \xrightarrow{2H^+,2e^-} GC$$
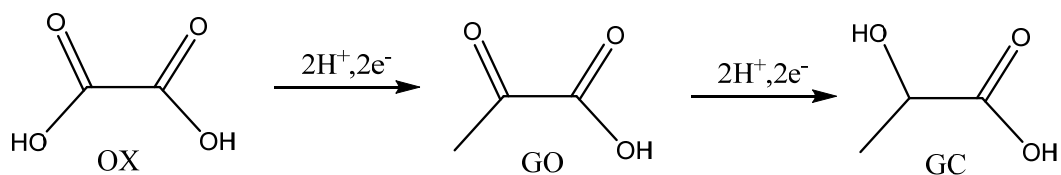
The electrocatalytic reduction of oxalic acid to produce glyoxylic acid (GO), the first intermediate deriving from a two-electron reduction, have been already commercialized. In fact, GO is an important C2 building block for many organic molecules of industrial importance, used in the production of agrochemicals, aromas, cosmetic ingredients, pharmaceutical intermediates and polymers. GO finds application in personal care as neutralizing agent, particularly in hair straightening products (shampoos, conditioners, lotions, creams). However, this electrosynthesis processes has many issues related to the easily deactivation of lead used as cathode material.

Therefore, novel cathode materials are highly desirable (Zhao et al., 2013). Hence the interest towards new sustainable electrocatalytic processes and the research & development of innovative electrode materials, and especially those able to selectively produce either GO or GC. There are still limited studies in this direction, among them can be cited the work by Sadakiyo et al. (2017) that obtained faradaic efficiencies (FE) at the best to GC below 50% (at room temperature) by using a porous anatase TiO_2 directly grown on Ti mesh or Ti felt as a cathode, but using a costly anode electrode (IrO_2/C) for oxygen evolution. Furthermore, high applied voltages (2.4 eV) were necessary. Zhao et al. (2013) showed that roughened TiO_2 film electrodes prepared by an anodic oxidation method are selective materials in OX reduction, with selectivity to GO (rather than to GC) up to about 55%, but at very high cell voltage (3.3 V).

We will report here results on the electrocatalytic reduction of OX to GO and GC by new electrodes based on g-C_3N_4 decorated TiO_2 nanotube ordered thin films (TiO_2-NTF) prepared by anodic oxidation. By controlling the method of deposition of g-C_3N_4 on TiO_2-NTF it is possible to change the selectivity, significantly increasing the FE up to 76% at low applied potential (-1.3 V). Although the mechanism of action should be further investigated, these results open new perspectives in the novel path of synthesis high-added-value chemicals such as GC from CO_2 via OX intermediate production.

Graphitic carbon nitride (g-C_3N_4) is an interesting nanocarbon material (Su et eal., 2013), with a layered structure similar to graphite, but having as basic structural unit either triazine or heptazine cores consisting of C and N atoms, similar with a layer of hexagonal carbon rings as in carbon materials (Inagaki et al., 2019).

2. Experimental

2.1 Materials

The g-C_3N_4/TiO_2-NTF composites have been prepared in a two-step process according to a procedure described in detail by Passalacqua et al., 2021. In the first step it was realized the synthesis of TiO_2-TNF by controlled anodic oxidation (AO) of a Ti foil (Passalacqua et al., 2014). Their preparation was made in a stirred electrochemical cell working at room temperature and containing ethylene glycol, 0.3 wt % NH_4F, and 2 vol. % H_2O. A titanium disc (0.025 mm thickness, 35 mm diameter, 99.96% purity, Alfa Aesar) was first cleaned by sonication in deionized water, acetone and isopropyl alcohol, sequentially, dried in air stream and finally anodized at 50V for 1h. As a result, self-organized TiO_2 nanotube layers were grown on both sides of the metallic disc, which however, remain and provides the substrate conductivity to operate as electrode. In the second step, the TiO_2-NTF was decorated with g-C_3N_4 by a direct chemical vapor deposition (CVD) method using melamine, urea or a 1:1 mixture of melamine-urea as precursor. Briefly, a certain amount of precursor (6, 12, 18, 24·10^{-3} mol) was put in a cleaned ceramic crucible with the anodized disc used as a cover. Then the crucible was heated (heating and cooling rate 5 °C/min) in a muffle in air at 550 °C for 3h. The investigated samples and their characteristics of preparation are collected in Table 1.

Table 1: Investigated samples and their characteristics

Sample name	Chemical components	AO parameters	g-C$_3$N$_4$ precursor
TiNT	TiO$_2$/Ti (TiO$_2$-NTF)	50 V; 1h	---
TiNTM6	g-C$_3$N$_4$-TiO$_2$/Ti	50 V; 1h	Melamine 6·10^{-3} mol
TiNTM12	g-C$_3$N$_4$-TiO$_2$/Ti	50 V; 1h	Melamine12·10^{-3} mol
TiNTM18	g-C$_3$N$_4$-TiO$_2$/Ti	50 V; 1h	Melamine 18·10^{-3} mol
TiNTM24	g-C$_3$N$_4$-TiO$_2$/Ti	50 V; 1h	Melamine 24·10^{-3} mol
TiNTU6	g-C$_3$N$_4$-TiO$_2$/Ti	50 V; 1h	Urea 6·10^{-3} mol
TiNTU12	g-C$_3$N$_4$-TiO$_2$/Ti	50 V; 1h	Urea 12·10^{-3} mol
TiNTU18	g-C$_3$N$_4$-TiO$_2$/Ti	50 V; 1h	Urea 18·10^{-3} mol
TiNTU24	g-C$_3$N$_4$-TiO$_2$/Ti	50 V; 1h	Urea 24·10^{-3} mol
TiNTMU6	g-C$_3$N$_4$-TiO$_2$/Ti	50 V; 1h	1:1 Melamine-Urea 6·10^{-3} mol
TiNTMU12	g-C$_3$N$_4$-TiO$_2$/Ti	50 V; 1h	1:1 Melamine-Urea 12·10^{-3} mol
TiNTMU18	g-C$_3$N$_4$-TiO$_2$/Ti	50 V; 1h	1:1 Melamine-Urea 18·10^{-3} mol
TiNTMU24	g-C$_3$N$_4$-TiO$_2$/Ti	50 V; 1h	1:1 Melamine-Urea 24·10^{-3} mol

2.2 Electrochemical setup

Figure 1 reports the sketch of the electrochemical cell used to study OX reduction reaction. The electrochemical cell is divided into two compartments, the anodic and the cathodic side, through a proton-exchange membrane (Nafion® 115). A 0.2 M Na$_2$SO$_4$ solution containing 0.03 M of OX (pH=2) was used in the cathodic compartment, while the electrolyte solution (0.2 M Na$_2$SO$_4$) was used for the anodic one.
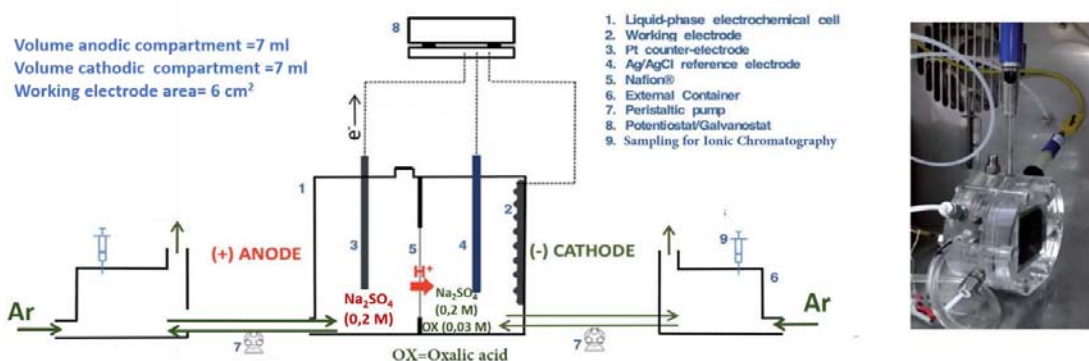

Figure 1: Experimental setup of the electrochemical cell for OX reduction

Before starting the reaction, the external reservoirs containing the electrolytic solutions were flowed with Argon to eliminate O$_2$. A peristaltic pump was used to flow the electrolytic solutions (flow rate 50 mL/min) to both the compartments of the cell.The amperometric detection (AD) experiments were made on the electrocatalysts reported in Table 1 serving as working electrode (WE). Electrode geometric area was about 5.7 cm^2. A constant voltage of -1.1 and -1.3 V vs Ag/AgCl was applied, recording the resulting current densities. A typical test was carried out for 2 hours at each investigated potential. The cathode side solution was analysed by Ionic Chromatography.

2.3 Characterization

XPS measurements were made on the electrocatalysts by using PHI Versa Probe II equipment (Physical Electronics). The spectra were recorded using Al Kα (1486.6 eV) X-ray source and an analyser pass energy of 23.5 eV and 117 eV for the high-resolution core level spectra and for the survey spectrum, respectively. The X-ray beam size was 100 microns at high power 100 W. The XPS peaks were calibrated with respect to a reference gold foil. The binding energy (BE) of the Au 4f$_{7/2}$ level was set to 84.0 eV.

3. Results and discussion

g-C_3N_4/TiO_2-NTF composites are characterized by a graphite-C_3N_4 dispersed patches deposited on the TiO_2 nanotubes array. They were characterized by various physico-chemical techniques (see Passalacqua et al., 2021) with reference to their use as photocatalysts.
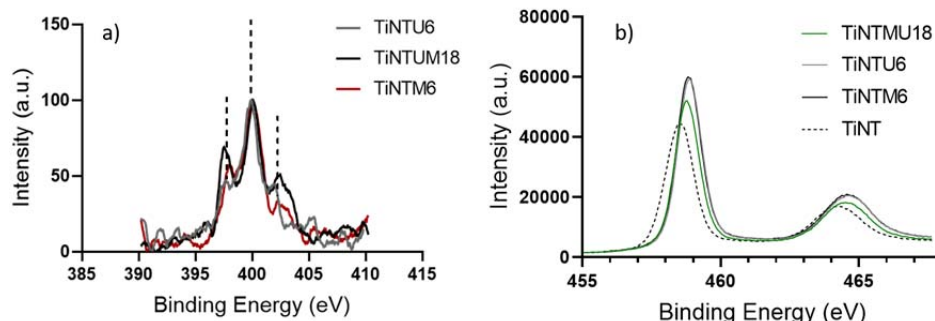

Figure 2: a) N1s and b) Ti2p XPS spectra for the composite materials, respect to the pristine TiNT

A survey XPS spectrum of the g-C_3N_4/TiO_2 composites indicated the presence of Ti, O, C and a small amount of N confirming the preparation. For all the investigated samples the weight percentage for Nitrogen is less than 1% wt. Figure 2a and 2b report the N1s and Ti2p spectra for some of the obtained composite materials, in particular for TiNTU6, TiNTM6 and TiNTUM18.

The N1s spectra, reported in Figure 2a, show three components assigned to pyridine-like C=N species (N1 species at 398.5 eV), conjugated amine C=N-H species (N2 at 399.9 eV), quaternary N (N3 at 401 eV). This assignment is consistent with the literature (Large et al., 2020) and indicates that the investigated material is a dispersed heptazine-based carbon nitride covering the TiO_2 nanotubes array.

The Ti2p spectra, Figure 2b, is also reported for same samples and compared with the reference TiO_2 nanotubes array (TiNT). In all the composite materials a shift with respect to pristine TiNT can be observed, indicating an interaction between the g-C_3N_4 and TiO_2 nanotubes. The results, however, are dependent on the use of a single or mixed precursor. The shift observed for the TiNTU6 and TiNTM6 is similar, about 0.21 eV respect to the reference TiNT, while for the TiNTUM18 sample the main peak of Ti2p is shifted of 0.10 eV respect to the TiN T reference sample. Due to low amount of N and thus signal intensity, a decomposition of N1s peak in components is not feasible. However, the shift observed for the Ti2p spectra in the composite materials with respect to TiNT suggests that the different interaction between TiO_2 nanotubes and g-C_3N_4 is achieved depending on the used precursor.

The electrodes reported in Table 1 have been studied in OX reduction reaction by using the electrochemical set up described in section 2.2. The OX is first reduced to glyoxylic acid ($C_2H_2O_3$, GO) through a two-electron reduction, and then Glycolic acid ($C_2H_4O_3$, GC) is produced from GO through a further two-electron reduction.

An overview of the results is reported in Figure 3 at both values of applied potential (-1.1 V, and -1.3 V vs Ag/AgCl). The faradaic efficiencies FE after 2 hours of reaction for each investigated potential are reported and compared to those obtained by the pristine TiO_2 nanotubes (TiNT).
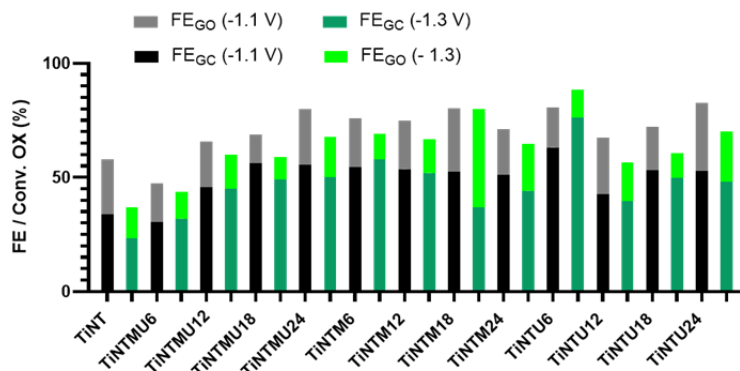

Figure 3: Efficiency to glyoxylic and glycolic acid of g-C_3N_4/TiO_2 composites and TiNT reference sample at the potential of -1.1 V and -1.3 V after 2 h of reaction.

The pristine TiO$_2$ (TiNT) shows a comparable faradaic efficiency to GO (FE$_{GO}$) and GC (FE$_{GC}$), with yields of about 24%, and 34%, respectively. After deposition of g-C$_3$N$_4$, an increase of FE$_{GC}$ is generally observed, while FE$_{GO}$ remains either similar or decreases with respect to the pristine TiNT, except for the TiNTM18 sample, at the applied potential of -1.3 V. This sample shows a FE$_{GO}$ about three times higher with respect to the pristine TiNT.

The best performances in terms of FE were obtained at an applied potential of -1.1 V, except for the TiNTU6 which show the highest FE$_{GC}$ =76% and very low FE$_{GO}$ =12% at the applied potential of -1.3 V. The effect of the use of different precursors, in terms of best performances, can be summarized as follows:

TiNTU6 > TiNTMU18 > TiNTM6

The best results were obtained at -1.1 V in the case of the TiNTU6 sample with a FE$_{GC}$ up to 63% and a FE$_{GO}$ lowered to 17%, although the performances are like the TiNTM6 (FE$_{GC}$ =58%; FE$_{GO}$ =12%).

These results highlight the capability of the g-C$_3$N$_4$ dispersed layer to tune the selectivity of the composite materials favouring the GC as the main product of reaction. Note, however, that the use of g-C$_3$N$_4$ alone, deposited directly on a Ti plate, does not result active, but studies are in progress to understand better the properties of g-C$_3$N$_4$ as electrode in OX electrocatalytic reduction.

The current density for the composite materials (displaying only those showing the best performances as a function of the precursor) are slightly worsen with respect to the pristine TiNT (Figure 4), remarking that g-C$_3$N$_4$ acts mainly as a modifier of selectivity, rather than itself as a catalytic element.
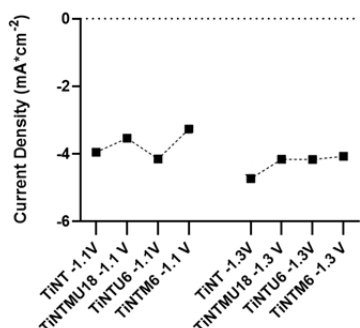

Figure 4: Current density for the TiNT and the composite electrodes (those with the best performances depending on the precursor TiNTU6 >TiNTMU18 >TiNTM6) at both the investigated applied potentials (-1.1 V and -1.3 V)

The Figure 5 reports the FE$_{GO}$ and FE$_{GC}$ together with the OX conversion as a function of the different precursors used in the preparation and their concentrations in the range $6 \cdot 10^{-3} \div 24 \cdot 10^{-3}$ mol.
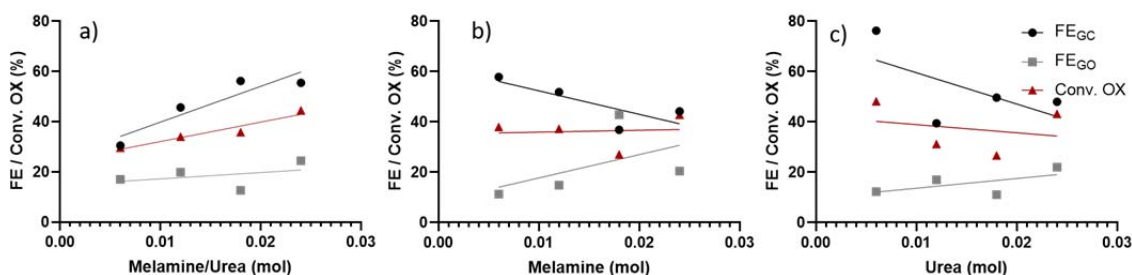

Figure 5: Correlation attempts between FE$_{GO}$, FE$_{GC}$ and oxalic acid conversion as a function of precursor concentration for the different used precursors, a) Melamine/Urea, b) Melamine, and c) Urea

Figure 5a shows the correlation for the MU (melamine/urea) precursor. Both FE$_{GC}$ and conversion of OX increase by increasing the MU precursor concentration, whilst the FE$_{GO}$ remains about constant. This means that in this specific case, new selective sites are created on increasing the MU precursor concentration.

For the U (urea) and M (melamine) precursors, Figures 5b and 5c, respectively, an opposite trend was observed. By increasing the M or U concentration the FE$_{GC}$ decreases while EF$_{GO}$ increases, suggesting that when a single precursor is used a very low concentration is required for tuning the selectivity to GC. U precursor at the lowest concentration results more effective.

XPS results indicate that the nature of the N species depends on the concentration and nature of the precursor, but further studies are in progress to correlate the nature of the species to those active in the electroreduction of OX to either GC or GO. Note, that with respect to the results presented by Zhao et al. (2013) that correlated the selectivity to GO to the presence of $TiO_2/Ti(OH)_3$ redox couple, our results are not currently supporting this interpretation, even if further studies are necessary. The behavior seems instead to be associated to the nature of the N inside the aromatic rings of g-C_3N_4 decorating patches, and how it affects the electronic properties of the TiO_2-NTF material. Further investigation by XPS are currently ongoing to correlate the properties to the amount of deposited g-C_3N_4 species.

4. Conclusions

The results confirm the capability of the graphite-C_3N_4 dispersed layer of the composite materials to tune the selectivity favouring the GC as the main product in the oxalic acid reduction reaction. In particular, the sample TiNTU6 (obtained by using the lower urea concentration of $6 \cdot 10^{-3}$ mol), shows the highest FE_{GC} of 76% while the FE_{GO} is lowered to 12%, with respect to the pristine TiO_2 (TiNT) showing faradaic efficiency to GO (FE_{GO}) and GC (FE_{GC}) of about 24%, and 34%, respectively.

XPS results indicate that the interaction between the g-C_3N_4 and TiO_2 nanotubes strongly depends on the precursor and its concentration, suggesting that the performances in the electroreduction of oxalic acid depend on this factor. These results are quite encouraging, considering that similar values can be usually achieved only at a higher applied potential (Fukushima et al., 2020; Yamauchi et al., 2019).

These finding have been useful to identify cathodic materials with characteristics suitable for electrocatalytic reduction of oxalic acid starting from different precursors.

References

Fukushima, T., Higashi, M., Kitano, S., Sugiyama, T. & Yamauchi, M., 2020, Multiscale design for high-performance glycolic acid electro-synthesis cell: Preparation of nanoscale-IrO_2-applied Ti anode and optimization of cell assembling, Catalysis Today, 351, 12–20.

Inagaki, M., Tsumura, T., Kinumoto, T., Toyoda, M., 2019, Graphitic carbon nitrides (g-C_3N_4) with comparative discussion to carbon materials, Carbon, 141, 580-607.

Large A.I., Wahl S., Abate S., Da Silva I., Jaen J.J.D., Pinna N., Held G., Arrigo R., 2020, Investigations of Carbon Nitride-Supported Mn_3O_4 Oxide Nanoparticles for ORR, Catalysts, 698, 1–19.

Murcia Valderrama, M. A., van Putten, R. J. & Gruter, G. J. M., 2019, The potential of oxalic – and glycolic acid based polyesters (review). Towards CO_2 as a feedstock (Carbon Capture and Utilization – CCU), European Polymer Journal, 119, 445–468.

Passalacqua R., Ampelli C., Perathoner S., Centi G., 2014, Self-standing TiO_2 nanotubular membranes for sustainable production of energy, Chemical Engineering Transactions, 41, 319–324.

Passalacqua R., Perathoner S., Centi G., 2020, Enhanced composites behaviour by coupling graphitic-C_3N_4 and titania nanotube array, Chemical Engineering Transactions, 84, submitted.

Perathoner S., Centi G., 2019, Catalysis for solar-driven chemistry: the role of electrocatalysis, Catalysis Today 330, 157-170.

Sadakiyo, M., Hata, S., Cui, X., Yamauchi, M., 2017, Electrochemical Production of Glycolic Acid from Oxalic Acid Using a Polymer Electrolyte Alcohol Electrosynthesis Cell Containing a Porous TiO_2 Catalyst, Scientific Reports, 7, 17032.

Su, D.S., Perathoner, S., Centi, G., 2013, Nanocarbons for the Development of Advanced Catalysts, Chemical Reviews, 113, 5782–5816.

Yamauchi, M., Hata, S., Eguchi, H., Kitano, S., Fukushima, T., Higashi, M. Sadakiyo, M., Kato, K., 2019, Catalytic enhancement on Ti-Zr complex oxide particles for electrochemical hydrogenation of oxalic acid to produce an alcoholic compound by controlling electronic states and oxide structures, Catalysis Science & Technology, 9, 6561–6565.

Zhao, F., Yan, F., Qian, Y., Xu, Y. & Ma, C., 2013, Roughened TiO_2 film electrodes for electrocatalytic reduction of oxalic acid to glyoxylic acid, Journal of Electroanalytical Chemistry, 698, 31–38.